C. S. Fraser†
L. Gruendic*
Division of Surveying Engineering
The University of Calgary
Calgary, Alberta T2N 1N4, Canada

The Analysis of Photogrammetric Deformation Measurements on Turtle Mountain

High-precision aerial photogrammetry has been employed to measure sub-centimetre rock displacements on the crown of the Frank Slide.

Abstract: *A high-precision photogrammetric deformation monitoring system has been developed and implemented, whereby low-level aerial photography is used for the detection of rock movements on the South Peak of Turtle Mountain, Alberta. Thus far, two epochs of measurement have been carried out. In this paper the deformation analysis of this photogrammetric network data is reported. Aspects discussed include the network adjustment and deformation analysis approaches adopted, with special emphasis being given to the point movement localization procedure. The analysis results, which confirm that the system is capable of detecting multi-point sub-centimetre movements on the crown of the Frank Slide, are presented.*

Introduction

Just over 80 years ago, in the Crowsnest Pass in southern Alberta, there occurred the famous Frank Slide. This major landslide comprised some 30 million cubic metres of rock, which moved down the east face of Turtle Mountain and buried a town and approximately three square kilometres of the surrounding Crowsnest Valley to an average depth of about 14 m. The remains of the Frank Slide, as they appear today, are shown in Figure 1. It is noteworthy that the summit of Turtle Mountain is about 1000 m above the valley floor. For geological and geotechnical details of the Frank Slide, the reader is referred to Cruden and Krahn (1978).

Since 1933, a number of deformation monitoring surveys have been carried out at the crown of the Frank Slide. In recent years these *in-situ* displacement measurements have been directed at ascertaining the stability of a five million cubic metre rock wedge which comprises the South Peak area of Turtle Mountain. The principal geotechnical hypothesis regarding the potentially hazardous movement of this pyramid block is that it will move eastward, thus causing a dilation at the gaping fissure which defines the western edge of the wedge. This fissure, called Crack 1, is shown in Figure 2. Although the crack monitoring scheme implemented is capable of detecting movements to a high accuracy, it does display a few drawbacks. First, only movement across or along Crack 1 can be monitored, and second, if hazardous movements occur, and these indicate potential structural failure, it will no longer be possible to safely carry out *in-situ* measurements.

High-precision photogrammetry is a measuring tool which is well suited to a deformation monitoring task such as Turtle Mountain, because it is both non-contact in nature and also capable of yielding a comprehensive picture of the rock displacement pattern over the entire summit ridge area. At the invitation of the Alberta Department of the Environment, the first author conducted a comprehensive study to ascertain whether analytically restituted low-level aerial photography could be used to measure sub-centimetre rock movements on the South Peak. This investigation, the details of which have been reported in Fraser (1983), embraced photogrammetric network design and diag-

† Presently with Geodetic Services, Inc., 1511 Riverview Drive, Melbourne, FL 32901.

* On leave from The Institute of Applied Geodesy, University of Stuttgart, 7000 Stuttgart 1, Federal Republic of Germany.

Photogrammetric Engineering and Remote Sensing,
Vol. 51, No. 2, February 1985, pp. 207-216.
0099-1112/85/5102-0207$02.25/0
© 1985 American Society of Photogrammetry

FIG. 1. Turtle Mountain and The Frank Slide, Alberta (photo by C. Beaty).

nosis, as well as sensitivity analysis. From the results of the study it was concluded that a photogrammetric measuring system was a feasible option for monitoring deformations on Turtle Mountain. Consequently, the decision was made to develop and implement such a system.

A general overview of the photogrammetric monitoring system developed has been given in Fraser and Stoliker (1983). In the present paper, aspects of the deformation analysis approach employed in the system are detailed. Also, the results obtained from a two-epoch analysis of the photogrammetric measurements thus far carried out are reported. The emphasis of the paper is on describing the point-movement localization procedure adopted. Prior to addressing this topic, however, the network adjustment approach used, and results of the photogrammetric block adjustments, are discussed.

PHOTOGRAMMETRIC NETWORKS

DATA ACQUISITION

Through an analytical pre-analysis procedure it was determined that satisfactory network precision and sensitivity would be obtained from an aerial photographic coverage comprising six or more images at a scale of close to 1:2000, with all the 20 to 30 monitoring points appearing on each of the photographs (Fraser, 1983). In the summer of 1982 an object target array of 24 points was established on the summit ridge of Turtle Mountain. It was impractical to install more targets because of the highly weathered and fractured state of the surface limestone rock. The positions of the 19 targets subsequently used in the deformation analysis are shown in Figure 2. The network of object points was then imaged on two occasions, with the two epochs of observation being one year apart. A standard mapping camera of 152-mm focal length was used for the photography, which was imaged at scales ranging from about 1:2200 to 1:2800. The exposure station locations at epochs 1 and 2 are shown in Figure 3.

The same camera, a Wild RC8, was used on the two photographic missions, and every attempt was made at epoch 2 to recapture the imaging configuration of epoch 1. However, the extremely difficult flying conditions encountered meant that this goal could only be partially achieved. Also, due to excessive turbulence, the design imaging scale of 1:2000 was not achieved at either epoch. A subsequent analysis of the network at epoch 1 did, however, indicate sufficient sensitivity to detect multipoint sub-centimetre movements (Fraser and Stoliker, 1983). From the strips of photography flown

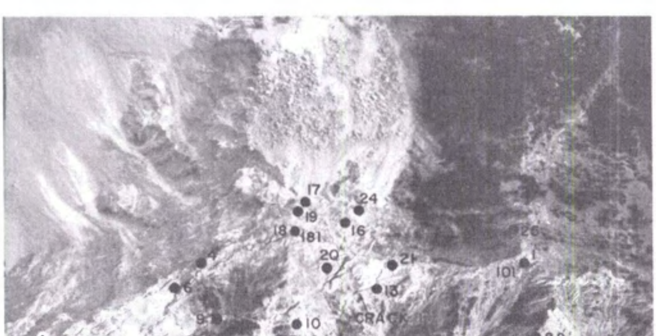

FIG. 2. Object target point array on the summit ridge.

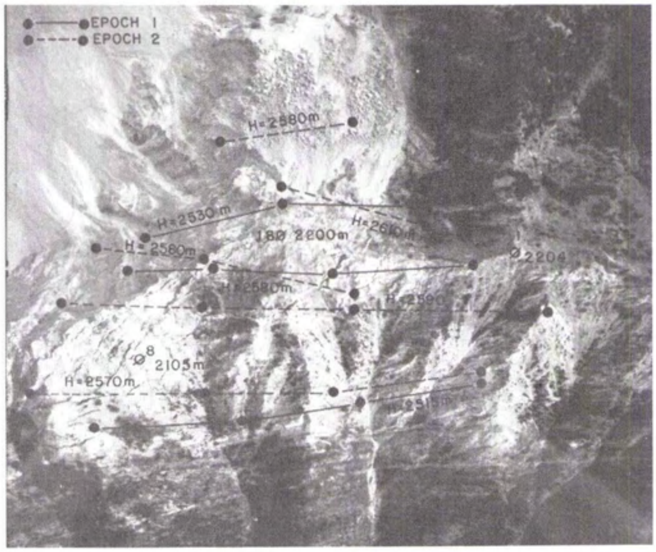

FIG. 3. Exposure station configurations at epochs 1 and 2.

in August, 1982, eleven exposures were included in the photogrammetric network for epoch 1. Not all targets were imaged on all photographs, but at least six imaging rays were available for space intersection at each object point. In order to enhance the geometric strength of the imaging configuration at epoch 2, four additional exposures from the 1983 photography were used, thus yielding a 15-photo network.

Image coordinate measurements were carried out monoscopically in a Wild AC/1 analytical plotter. Multiple readings of each point were made on the original film negatives, to an estimated standard error of about two micrometres.

ADJUSTMENT OF PHOTOGRAMMETRIC NETWORKS

For the purpose of the photogrammetric monitoring, all points were considered to lie on a potentially deformable body. In such a situation the establishment of an object space control field is precluded and the deformation monitoring network becomes one of "relative" type. In solving the datum or zero-order design problem, a free-network adjustment approach, namely, the method of inner-constraints (e.g., Meissl, 1969; Blaha, 1971), has been adopted. Under this scheme the solution for the photogrammetric bundle adjustment can be written as

$$\begin{pmatrix} \mathbf{x}_1 \\ \mathbf{x}_2 \\ \mathbf{k} \end{pmatrix} = \begin{pmatrix} \mathbf{A}_1^T\mathbf{P}\mathbf{A}_1 & \mathbf{A}_1^T\mathbf{P}\mathbf{A}_2 & 0 \\ & \mathbf{A}_2^T\mathbf{P}\mathbf{A}_2 & \mathbf{G} \\ & & 0 \end{pmatrix}^{-1} \begin{pmatrix} \mathbf{A}_1^T\mathbf{P}\boldsymbol{\ell} \\ \mathbf{A}_2^T\mathbf{P}\boldsymbol{\ell} \\ 0 \end{pmatrix} \quad (1)$$

where $\mathbf{x}_1$ and $\mathbf{x}_2$ are the parameter estimates relating to the exterior orientation and additional parameters, and the object target point coordinates, respectively; $\mathbf{A}_1$ and $\mathbf{A}_2$ are the corresponding configuration matrices; $\mathbf{P}$ is the image coordinate weight matrix; $\boldsymbol{\ell}$ is the observational discrepancy vector; $\mathbf{k}$ is a vector of Lagrangian multipliers; and $\mathbf{G}$ is a similarity transformation matrix, where $\mathbf{A}_2\mathbf{G} = 0$. For an object point j, in a network with a datum defect of seven, the appropriate 3 by 7 matrix $\mathbf{G}_j$ is given as

$$\mathbf{G}_j = \begin{pmatrix} 1 & 0 & 0 & 0 & Z_j & -Y_j & X_j \\ 0 & 1 & 0 & -Z_j & 0 & X_j & Y_j \\ 0 & 0 & 1 & Y_j & -X_j & 0 & Z_j \end{pmatrix}. \quad (2)$$

In the photogrammetric network adjustments conducted for the Turtle Mountain investigation the inner constraints imposed through $\mathbf{G}$ related in some cases to all object points and in others to a sub-set of targets. The former situation can be advantageous at the sensitivity analysis stage, because an optimum overall form of the cofactor matrix $\mathbf{Q}_{x_2}$ of object point XYZ coordinates is obtained, i.e., trace $\mathbf{Q}_{x_2} \rightarrow$ minimum. The choice of which sub-set of object points should be subjected to inner constraints in the datum assignment is very much dependent on the known or anticipated characteristics of the deformation field. If geotechnical hypotheses regarding the likely displacement patterns are available, then these can be considered in the datum definition. For example, one hypothesis regarding the South Peak of Turtle Mountain is that a block movement will occur across Crack 1. Additional hypotheses envisage smaller block movements within the pyramid wedge as gradual crack dilation takes place. Smaller segments of rock can then be expected to continue to peel away over time from the eastern side of the pyramid block. An appropriate selection of the datum assists in the examination of the deformation trends indicated by XYZ coordinate differences between measuring epochs.

However, it must be recalled that the initial selection of a datum has no impact on the testing of the global congruence of adjusted networks, so long as the computational base is the same for each epoch. In the monitoring system applied to Turtle Mountain, S-transformations of covariance matrices are employed, and, thus, one has considerable flexibility in assigning a zero-variance computational base. This aspect is further developed in the following section.

For each measuring epoch the photogrammetric block was adjusted according to Equation 1, with the datum being defined in terms of only those points on the western side of Crack 1. The results obtained, along with those of a subsequent combined adjustment, are presented in Table 1. Both the networks at epochs 1 and 2 exhibit the same level of precision, a mean positional standard error of $\bar{\sigma}_c \simeq \pm 4$ mm. Also, the homogeneity of precision, as expressed by the eigenvalue ratio, is roughly the same at each measuring epoch. The anticipated fall-off in overall accuracy, which should accompany the smaller image scale at epoch 2, appears to be effectively counterbalanced through an increased network strength provided by the additional four exposures.

Deformation Analysis

Phases of the Analysis

Central to any deformation analysis is the proof of the existence or non-existence of point movements. Because neither "true" coordinates nor "true" deformations can be obtained through a physical measuring process, it is necessary to turn to statistical testing of "estimated" deformations in order to establish whether significant movements have occurred between two measuring epochs. Generally, the formulated null hypothesis which is tested is that network points have not moved. If this hypothesis passes the linear hypothesis test at the chosen confidence level (usually 95 percent), the assumption that no significant deformation has occurred in the network shape (and, in some circumstances, size) is accepted. Essentially, the congruence of the two networks is examined within the tolerance implied by their respective covariance matrices.

Rejection of the null hypothesis indicates that significant deformations have occurred, and it is then necessary to examine the localized nature of the point movements. An examination of trends in the resulting strain field may also be warranted. The approach to deformation analysis adopted in the Turtle Mountain monitoring project is comprised of three interrelated phases:

- global congruency testing of the network,
- localization of deformations in space and time, and
- testing the network, if it has been deformed, for significant components of homogeneous strain.

In the following sections the former two of these phases are considered in detail, whereas the latter is only briefly touched upon. Only the appropriate analysis procedure for "relative" deformation networks is considered. One of the features of the deformation analysis approach adopted is the use of S-transformations (Baarda, 1973) for datum-to-datum transformation of both covariance matrices and the vector of XYZ coordinate differences. The deformation localization software package implemented in the Turtle Mountain monitoring system was developed by the second author and his colleagues at the University of Stuttgart (e.g., Gruendig *et al.*, 1982; 1983).

The Global Congruency Test

Fundamentally, this test examines the null hypothesis that the object target point array is stable over all measuring epochs. For the case of a two-epoch analysis, the null hypothesis H_0 can be written as

Table 1. Summary of Photogrammetric Free-Network Adjustment Results for Epochs 1 and 2, and the Combined Adjustment which Followed the Deformation Localization Procedure. Each Network has the Same Datum

	Epoch 1	Epoch 2	Epochs 1 + 2
• Average image scale	1 : 2 300	1 : 2 680	1 : 2 550
• Number of photographs	11	15	26
• Number of object points	20	19	29
• RMS value $s_{x,y}$ of image coordinate residuals	± 2.2 μm	± 2.1 μm	± 2.2 μm
• Mean standard errors: $\bar{\sigma}_c$	± 4.1 mm	± 3.9 mm	± 3.4 mm
$\bar{\sigma}_{X,Y}$	± 2.9 mm	± 2.7 mm	± 2.3 mm
$\bar{\sigma}_Z$	± 5.8 mm	± 5.6 mm	± 5.1 mm
• Square root of the ratio of the largest over the smallest eigenvalue of $\mathbf{Q}_{x_2}$	8.7	9.1	8.4
• Degrees of freedom	223	312	552

$$H_0\text{: } \mathrm{E}\{\mathbf{x}_2^{(i+1)}\} - \mathrm{E}\{\mathbf{x}_2^{(i)}\} = \mathrm{E}\{\mathbf{d}\} = 0 \tag{3}$$

where $\mathbf{x}_2^{(i)}$ is the vector of XYZ object point coordinates at epoch i, and $\mathbf{d}$ is the vector of coordinate differences. A standard F-test, in which the quadratic form of the deformations is compared to the *a posteriori* variance factor, determines whether H_0 will be rejected (e.g., Pelzer, 1971; Niemeier, 1981).

In order to implement the congruency test, both the vectors $\mathbf{x}_2^{(i)}$ and the cofactor matrices $\mathbf{Q}_{x_2}^{(i)}$ must refer to a common datum, which is generally defined in terms of the points common to each epoch. Hence, if an arbitrary datum has been used for the calculation of $\mathbf{Q}_{x_2}$ and $\mathbf{x}_2$, a datum transformation may need to be applied prior to the congruency testing. To transform $\mathbf{x}_2$ and $\mathbf{Q}_{x_2}$ to the required computational base, the following partitioning scheme is first adopted:

$$\mathbf{x}_2 = \begin{pmatrix} \mathbf{x}_{2r} \\ \mathbf{x}_{2e} \end{pmatrix} \text{ and } \mathbf{Q}_{x_2} = \begin{pmatrix} \mathbf{Q}_{x2r} & \mathbf{Q}_{x2re} \\ \text{symm.} & \mathbf{Q}_{x2e} \end{pmatrix} \tag{4}$$

where the subscripts r and e stand for "retain" and "eliminate." An S-transformation is then applied as follows:

$$\mathbf{x}_{2sr} = \mathbf{S}\ \mathbf{x}_{2r} \tag{5}$$

and

$$\mathbf{Q}_{x_{2s}} = \mathbf{S}\ \mathbf{Q}_{x_2}\mathbf{S}^{\mathrm{T}} \tag{6}$$

where

$$\mathbf{S} = \mathbf{I} - \mathbf{G}(\mathbf{G}^{\mathrm{T}}\mathbf{G})^{-1}\overset{*}{\mathbf{G}}{}^{\mathrm{T}},\ \mathbf{G} = \begin{pmatrix} \mathbf{G}_r \\ \mathbf{G}_e \end{pmatrix} \text{ and } \overset{*}{\mathbf{G}} = \begin{pmatrix} \mathbf{G}_r \\ 0 \end{pmatrix} \tag{7}$$

The matrices $\mathbf{G}$ and $\overset{*}{\mathbf{G}}$ are composed of the same elements as indicated by Equation 2, but they too are partitioned according to the scheme of Equation 4. For further details on the S-transformation as it relates to deformation monitoring, the reader is referred to van Mierlo (1981). The implementation of covariance transformations described here follows the method proposed by Strang van Hees (1982). Because only the cofactor matrix $\mathbf{Q}_{x_{2sr}}$ relating to $\mathbf{x}_{2sr}$ is required for subsequent testing, Equation 6 can be simplified somewhat to

$$\mathbf{Q}_{x_{2sr}} = (\mathbf{I} - \mathbf{G}_r(\mathbf{G}_r^{\mathrm{T}}\mathbf{G}_r)^{-1}\mathbf{G}_r^{\mathrm{T}})\ \mathbf{Q}_{x_{2r}}\ (\mathbf{I} - \mathbf{G}_r(\mathbf{G}_r^{\mathrm{T}}\mathbf{G}_r)^{-1}\mathbf{G}_r^{\mathrm{T}}) \tag{8}$$

Once $\mathbf{x}_{2sr}^{(i)}$ and $\mathbf{Q}_{x_{2sr}}^{(i)}$ are obtained for each epoch i, the congruency testing can take place. It is, of course, possible to circumvent the S-transformation procedure at the global congruency test stage by simply ensuring that the inner-constraint datum assigned to the network adjustment at each epoch comprises the same sub-set of object points. This was the case with the Turtle Mountain photogrammetric networks. For scale equalization between the networks at the two epochs, the appropriate column rank of $\mathbf{G}$ had to be changed to 6 for the application of Equation 5 in the transformation for the first epoch; but the rank remained 7 for the second epoch.

In the congruency test, the test value ω is computed from the expression

$$\omega = \frac{\Omega}{h\sigma_0^2} = \frac{\mathbf{d}^{\mathrm{T}}\mathbf{Q}_d^{+}\mathbf{d}}{h\sigma_0^2} \tag{9}$$

where

$$\mathbf{d} = \mathbf{x}_{2sr}^{(2)} - \mathbf{x}_{2sr}^{(1)} \tag{10}$$

and

$$\mathbf{Q}_d = \mathbf{Q}_{x2sr}^{(2)} + \mathbf{Q}_{x2sr}^{(1)} \tag{11}$$

The cofactor matrix $\mathbf{Q}_d$ of coordinate differences has a rank of h, and the common variance factor σ_0^2 can be estimated from

$$\sigma_0^2 = (r^{(1)}\sigma_{01}^2 + r^{(2)}\sigma_{02}^2)/r \tag{12}$$

where $r = r^{(1)} + r^{(2)}$, $r^{(i)}$ being the degrees of freedom in network i, and σ_{0i}^2 is the corresponding variance factor. The pseudo-inverse in Equation 9 is necessitated because of the rank defect of $\mathbf{Q}_d$.

The test of ω is against the Fisher value $F_{h,r,1-\alpha}$, and a significance level of $\alpha = 0.05$ is typically selected. Should ω be less than this critical value, the null hypothesis of no deformation is accepted. On the other hand, should the test fail, as it did for the two-epoch analysis of the Turtle Mountain photogrammetric data, the next task is to locate the point or points whose displacements caused the target array to significantly change in shape. For a multi-epoch analysis, a localization in the time domain is also required. The so-called Hannover approach (Niemeier, 1979; 1981) has been employed for this phase in the deformation analysis system developed. However, in this paper, we are only concerned with the two-epoch analysis case, so the location in time problem does not apply.

LOCALIZATION OF DEFORMATIONS

Congruency Testing of Partial Networks. As shown, for example, in Niemeier (1979), all information regarding the non-congruence of two object point networks is contained in the quadratic form Ω (see Equation 9). Thus, it is possible to examine the individual contribution Ω_j from each apparent point displacement $\mathbf{d}_j$. The point for which the maximum Ω_j component is found is then deemed to be the most significant movement, i.e., $\mathbf{d}_j = (dX_j, dY_j, dZ_j)^{\mathrm{T}}$ represents a significant deformation. Each value of Ω_j is readily computed by means of the following conformal partitioning procedure (see Niemeier (1979) and van Mierlo (1981)):
Let

$$\mathbf{d} = \begin{pmatrix} \mathbf{d}_r \\ \mathbf{d}_j \end{pmatrix} \text{ and } \mathbf{Q}_d^{+} = \begin{pmatrix} \mathbf{P}_r & \mathbf{P}_{rj} \\ \text{symm.} & \mathbf{P}_j \end{pmatrix} \tag{13}$$

then

$$\Omega_j = \bar{\mathbf{d}}_j^{\mathrm{T}} \mathbf{P}_j \bar{\mathbf{d}}_j \tag{14}$$

where

$$\bar{\mathbf{d}}_j = \mathbf{P}_j^{-1} \mathbf{P}_{rj} \mathbf{d}_r + \mathbf{d}_j \tag{15}$$

Following the location of the point displacement which contributes most significantly to the non-congruence of the two target point networks, the question must be asked as to whether that point is the only one to have moved, or is the deformation field comprised of further point displacements. In order to answer this question, the influence of the first-located movement $\mathbf{d}_j$ must be eliminated from the network datum. This "elimination" procedure follows the same sequence as detailed in Equations 4 through 9. The vector $\mathbf{d}$ of deformations and the cofactor matrix $\mathbf{Q}_d$ are first partitioned as

$$\mathbf{d} = \begin{pmatrix} \mathbf{d}_r \\ \mathbf{d}_e \end{pmatrix} \text{ and } \mathbf{Q}_d = \begin{pmatrix} \mathbf{Q}_{dr} & \mathbf{Q}_{dre} \\ \text{symm.} & \mathbf{Q}_{de} \end{pmatrix} \tag{16}$$

where $\mathbf{d}_e$ is formed by the significant deformations. Following the detection of the first movement $\mathbf{d}_j$, $\mathbf{d}_e \equiv \mathbf{d}_j$ and $\mathbf{Q}_{de}$ is a 3 by 3 matrix relating to dX_j, dY_j, and dZ_j. An S-transformation is then carried out to remove the points in $\mathbf{d}_e$ from the computational base. Again,

$$\mathbf{G} = \begin{pmatrix} \mathbf{G}_r \\ \mathbf{G}_e \end{pmatrix} \tag{17}$$

which yields

$$\mathbf{S} = \begin{pmatrix} \mathbf{I} - \mathbf{G}_r(\mathbf{G}_r^{\mathrm{T}}\mathbf{G}_r)^{-1}\,\mathbf{G}_r^{\mathrm{T}} & 0 \\ - \mathbf{G}_e(\mathbf{G}_r^{\mathrm{T}}\mathbf{G}_r)^{-1}\,\mathbf{G}_r^{\mathrm{T}} & \mathbf{I} \end{pmatrix}. \tag{18}$$

The transformed deformation vector and cofactor matrix follow from

$$\begin{pmatrix} \mathbf{d}_{sr} \\ \mathbf{d}_{se} \end{pmatrix} = \mathbf{S} \begin{pmatrix} \mathbf{d}_r \\ \mathbf{d}_e \end{pmatrix} \tag{19}$$

and

$$\mathbf{Q}_{ds} = \mathbf{S}\,\mathbf{Q}_d\,\mathbf{S}^{\mathrm{T}}. \tag{20}$$

If there are k "eliminated" points in $\mathbf{d}_{se}$, the congruency test for the partial network formed by the "retained" object points is performed as

$$\frac{\mathbf{d}_{sr}^{\mathrm{T}}\,\mathbf{P}_{sr}\,\mathbf{d}_{sr}}{(h - 3k)\,\sigma_0^2} < F_{h-3k,r,1-\alpha} \tag{21}$$

where $\mathbf{P}_{sr}$ is the sub-matrix of $\mathbf{Q}_{ds}^{+}$ corresponding to $\mathbf{d}_{sr}$. The null hypothesis that the partial network has not changed in shape is accepted if the test, Equation 21, passes. Thus, the elements of $\mathbf{d}_{se}$ indicate the significant deformations with respect to the stable target point network described by $\mathbf{d}_{sr}$. If the congruency test fails, the point with the largest Ω_j component is again determined by means of Equation 14. The three corresponding coordinate differences dX, dY, and dZ are then added to the $\mathbf{d}_e$ vector, k is incremented by one, and both the S-transformation and the partial network test are repeated. At the completion of the deformation localization phase, $\mathbf{d}_{se}$ represents the vector of "actual"; deformations.

Having determined both the significant single-point displacements and the stable array of points, it is possible to test whether any sub-group of points underwent a significant block movement, e.g., a translation or rotation with respect to the partial network of stable points. This test can follow in much the same way as the procedure for localizing single-point movements detailed above, or, alternatively, a multi-dimensional t-test can be employed.

Testing of Deformations. Through the use of either multi- or single-dimensional t-tests, it is possible, in a sense, to confirm the findings of the deformation localization process. This confirmation is valuable because during the localization the existence of a movement of a group of points may affect the sequence of elimination of single points. In the presence of a group movement, it is conceivable that a stable point may be flagged as having undergone significant movement, because the hypothesis tested deals only with single-point displacements. Considering the single-point case, the formulated null hypothesis to be tested is that $\mathbf{d}_j = (dX_j, dY_j, dZ_j)^{\mathrm{T}} = 0$. This hypothesis is then examined by the test

$$\frac{\mathbf{d}_j^{\mathrm{T}}\,\mathbf{Q}_{d_j}^{-1}\mathbf{d}_j}{\sigma_0^2} < 3F_{3,r,1-\alpha} \tag{22}$$

where $\mathbf{Q}_{d_j}$ is the cofactor matrix of the displacement vector $\mathbf{d}_j$. One feature of photogrammetric networks subjected to inner-constraint adjustment is that there is generally only limited correlation both between the estimated XYZ coordinates of an object point, and between the coordinates of adjacent points. Thus, in practice, single-point t-tests according to Equation 22 can generally be applied. Further, in the presence of limited covariance, it is also possible to test the individual coordinate changes.

Combined Network Adjustment. Once it is ascertained which object points were subjected to movement between epochs 1 and 2, all the photogrammetric data can be combined into a single network adjustment. Points in epoch 2 at which significant deformation took place are assigned new numbers in the bundle adjustment. The resulting estimated distance between each of the newly numbered points and its corresponding position in epoch 1 (effectively a separate point) then indicates the magnitude of movement. If the displacement vector at any point lies outside the corresponding confidence ellipsoid, a significant movement is indicated (e.g., Heck, 1982). For a probability level of $1 - \alpha$, the semi-axes of the standard ellipsoids are multiplied by the factor $(3F_{3,r,1-\alpha})^{1/2}$.

It is quite possible that the vector of deformations resulting from the combined network will not exactly equal the final significant deformation vector $\mathbf{d}_{se}$ obtained by means of the localization process. Discrepancies can, however, be anticipated to be reasonably insignificant, so long as an appropriate datum of stable points is selected. It should be noted that "stable" in this sense implies that the points in question did not undergo significant movement, although they may have indeed been displaced by a less than detectable amount between measuring epochs 1 and 2.

Deformation Localization Results. The results of the deformation localization computations for the two-epoch analysis of photogrammetric measurements on Turtle Mountain are summarized in Table 2. The first eight points listed were found to have moved significantly, at a probability level of 0.95. The three points below the dashed line, on the other hand, displayed movements which were only marginally significant. In fact for points 11 and 12 the t-test passed.

The most significant single-point movement located was point 20, which was estimated to have been displaced by 6.3 cm in an approximate azimuth of 246°. As it turned out, this target was physically relocated by Alberta Environment personnel, and the extent of movement was not made available to the authors—indeed nor was the point number of the relocated point—until after the localization procedure was completed and the results reported. From surface distance measurements and a compass reading, it was determined that the target was shifted 6.2 cm in an azimuth of approximately 250°. Thus, the independent check on the photogrammetric measurement revealed a discrepancy of 1 mm, which is a surprisingly accurate result considering that the 95 percent confidence region associated with point 20 is approximately a circle of 5-mm radius in the horizontal plane. In the vertical the 95 percent region extends to about ±10 mm.

The deformations listed in Table 2 (see also Figure 4) indicate two likely group movements, which were also tested using the localization software. One is the block formed by points 4, 6, and 9, and the other is the group 16, 17, and 24. For both these groups, the hypothesis that there was no block movement with respect to the partial network of stable targets was rejected at the 0.05 significance level. The vertical slippage experienced by these two 3-point groups is consistent with the hypothesis that envisages smaller block movements of rock segments on the eastern side of the pyramid wedge.

Combined Adjustment Results. The findings of the localization process were that, while ten of the 19 common points remained stable, nine underwent a significant movement. Referring to Table 2, points 11 and 12 were deemed to belong to the stable group, whereas point 9 was classed as unstable, principally after consideration of its detected participation in a block movement. As a final confirmation of the deformation pattern indicated in Table 2, all photogrammetric data were combined into a single network of 26 photographs and 29 points (20 original and nine renumbered in the epoch 2 data).

Illustrated in Figure 4 are the deformations determined in the combined network adjustment, the statistical summary of which is listed in Table 1. Also shown in the figure are the resulting 95 percent confidence regions (error ellipses in the horizontal and a confidence interval in the vertical). Although minor discrepancies exist between the deformation pattern obtained in the localization process and the displacements shown in Figure 4, the point movements are in close overall agreement. A component of the difference in estimated deformations comes

TABLE 2. SIGNIFICANT DEFORMATIONS DETECTED IN THE LOCALIZATION RESULTS FOR EPOCH 2 VERSUS EPOCH 1. THE POINT MOVEMENTS, OF MAGNITUDE d, ARE LISTED IN THE ORDER IN WHICH THEY WERE LOCATED

Point Number	dX (cm)	dY (cm)	dZ (cm)	d (cm)	Significant Deformation at $\alpha = 0.05$? Localization	t-test
20	−5.0	2.1	−3.2	6.3	yes	yes
24	−1.3	0.1	−5.2	5.3	yes	yes
6	−2.4	−0.2	−2.0	3.2	yes	yes
17	−1.4	0.5	−2.9	3.3	yes	yes
25	−1.8	0.5	0.4	1.9	yes	yes
16	0.1	0.1	−4.4	4.4	yes	yes
13	0.4	0.9	−3.5	3.6	yes	yes
4	−1.2	−0.3	−2.4	2.7	yes	yes
11	0	0.1	−3.8	3.8	yes (marginal)	no
12	−0.9	0.4	−2.9	3.0	yes (marginal)	no
9	−0.9	−0.1	−2.2	2.4	yes (marginal)	yes

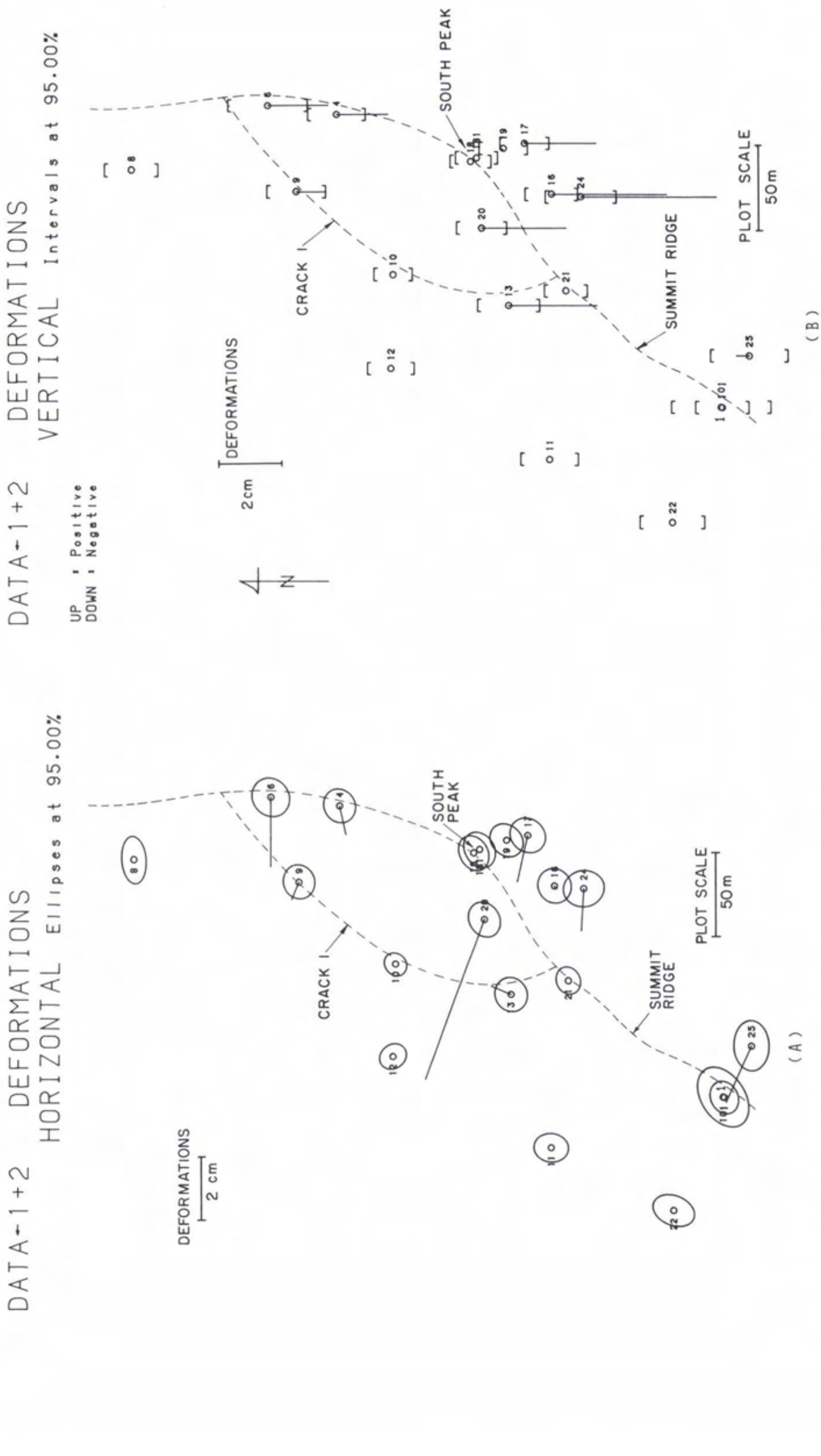

FIG. 4. Point movements between epochs 1 and 2, as determined in the combined network adjustment. (A) Horizontal deformations. (B) Vertical deformations.

from the inclusion of points 11 and 12 in the stable target array. Thus, the movement at these targets is constrained to zero in the combined network.

Strain Analysis. In the Turtle Mountain investigation it was initially thought that the determination of strain components would contribute to a better understanding of the mechanisms of any deformation that was detected, e.g., strain due to water pressure and flow. For the determination of the rates of homogeneous infinitesimal strain, the method proposed by Brunner (1979) was adopted. Under this approach deformations are assumed to result from an affine transformation in a homogeneous strain field which may cover either all or part of the object point network. The strain components of extensions along each coordinate axis and shear in each plane, and the components of rigid body rotation about each orthogonal axis, are then related to the estimated deformations **d** (coordinate differences) by

$$\mathbf{d} = \mathbf{B}\,\mathbf{u} \tag{23}$$

where **B** is the coefficient matrix of the incremental three-dimensional affine transformation (see Brunner (1979)) and **u** is the vector of strain parameters, given as

$$\mathbf{u}^{T} = (\epsilon_{XX}, \epsilon_{YY}, \epsilon_{ZZ}, \epsilon_{XY}, \epsilon_{XZ}, \epsilon_{YZ}, \omega_{XX}, \omega_{YY}, \omega_{ZZ}) \tag{24}$$

Extension along the k-axis is indicated by ϵ_{kk}, shear in the jk-plane by ϵ_{jk}, and rotation about the k axis by ω_{kk}. In the typical case where there are more than three object points, the method of least squares is adopted for the solution of **u**. Again, because of the defect of rank of the covariance matrix of **d**, a pseudo-inverse is used in the solution of the resulting normal equations: i.e.,

$$(\mathbf{B}^{T}\mathbf{Q}_{d}^{+}\mathbf{B})\mathbf{u} - \mathbf{B}^{T}\mathbf{Q}_{d}^{+}\mathbf{d} = 0. \tag{25}$$

From **u**, both principal strains and the volumetric strain can be computed. In conducting a strain analysis, it is useful to keep in mind that the vector of coordinate differences is a datum variant quantity, and so an appropriate datum must be selected. One obvious choice in this regard is the partial network of stable points which is identified by the deformation localization procedure. If the strain field is assumed to include all significant single-point deformations, the vector $\mathbf{d}_{se}$ from Equation 19 is used in Equation 25, with $\mathbf{P}_{se}$, the submatrix of $\mathbf{Q}_{ds}^{+}$ corresponding to $\mathbf{d}_{se}$, being substituted for $\mathbf{Q}_{d}^{+}$.

Following the computation of **u**, the null hypothesis of strain field homogeneity can be tested with an F-test analogous to the congruency test for significant deformation. Further, it is also possible to determine whether the strain components are statistically significant at a chosen confidence level. Because of the high correlation which can be encountered between the nine parameters forming **u**, it is often necessary to adopt multi-dimensional rather than one-dimensional tests to ascertain whether the estimated values of selected strain components are significantly different from zero.

The deformation field subjected to a strain analysis in the reported monitoring study comprised nine points on the pyramid block at the South Peak (point 20 was excluded). Perhaps not surprisingly, given the nature of the point movements, the analysis did not reveal the presence of statistically significant homogeneous strain components.

Conclusions

The basic criterion governing the design of the photogrammetric monitoring system for Turtle Mountain was that the deformation analysis procedure should be able to monitor multiple target point movements of one centimetre or greater. From the results obtained for measuring epochs 1 and 2, it can be concluded that the photogrammetric networks established were of sufficient sensitivity to meet the required accuracy criteria, even though their precision was slightly below the optimum design level. At a confidence level of 95 percent, nine statistically significant single-point deformations and two 3-point group movements were detected, the smallest single-point displacement being 1.9 cm. The relocation of point 20 provided the only independent check of the photogrammetric measuring accuracy, and here the photogrammetrically measured movement was within 1 mm of the "true" value.

The results of this investigation lend further weight to the contention that high-precision analytical photogrammetry provides an accurate non-contact, three-dimensional measuring tool which is ideally suited both to tasks such as the detection of deformations on Turtle Mountain, and to general structural deformation monitoring in geotechnical engineering. However, in "relative" deformation networks, especially, a successful monitoring system requires more than a precise method of spatial positioning; an effective and practical deformation analysis procedure is also essential. The method of deformation localization reported in this paper can be thought of as effectively a combination of the so-called Hannover and Karlsruhe approaches (e.g., Heck, 1982), with the added flexibility of being able to handle with ease free networks of different dimensions, datums, and rank defects (Gruendig *et al.*, 1982). This flexibility is afforded mainly through the incorporation of S-transformations.

Acknowledgments

This work has been supported through a research contract with the Research Management Division of Alberta Environment.

References

Baarda, W., 1973. *S-Transformations & Criterion Matrices*. Netherlands Geodetic Commission, Publ. on Geodesy, New Series 5, No. 1, Delft.

Blaha, G., 1971. *Inner Adjustment Constraints with Emphasis on Range Observations*. Dept. of Geodetic Science Report No. 148, Ohio State University, Columbus, 85 pp.

Brunner, F. K., 1979. On the Analysis of Geodetic Networks for the Determination of the Incremental Strain Tensor. *Survey Review*, Vol. 25, pp. 56-67.

Cruden, D. M., and J. Krahn, 1978. Frank Rockslide, Alberta, Canada. In: Voight, B. (Ed.) *Rockslides and Avalanches*, Vol. 1, Elsevier, Amsterdam.

Fraser, C. S., 1983. Photogrammetric Monitoring of Turtle Mountain: A Feasibility Study. *Photogrammetric Engineering and Remote Sensing*, Vol. 49, No. 11, pp. 1551-1559.

Fraser, C. S., and P. C. Stoliker, 1983. Deformation Monitoring of a Landslide Area by High-Precision Photogrammetry. Presented to FIG XVII International Congress, Sofia, Bulgaria, June 19-28.

Gruendig, L., J. Bahndorf, and M. Neureither, 1982. *LOCAL-A FORTRAN Package for Localization of Movements in One-, Two- and Three-Dimensional Networks*. IAGB, University of Stuttgart.

———, 1983. Zur Auswirkung von Beobachtungsfehlern auf Deformationen oder Deformationen als Beobachtungsfehler gedeutet. Presented to FIG Comm. 6 Meeting, Munich.

Heck, B., 1982. Report of the FIG Working Group on the Analysis of Deformation Measurements. Presented to the FIG Comm. 6 Meeting, Budapest.

Meissl, P., 1969. Zusammenfassung und Ausbau der inneren Fehlertheorie eines Punkthaufens. *Deutsche Geodätische Kommission*, Series A, 61, pp. 8-21.

van Mierlo, J., 1981. A Testing Procedure for Analysing Geodetic Measurements. In: Hallermann, L. (Ed.) *Proc. II Int. Symp. on Deformation Measurements by Geodetic Methods, Bonn, 1978*. Konrad Wittner, Stuttgart, pp. 321-353.

Niemeier, W., 1979. *Zur Kongruenz mehrfach beobachteter geodätische Netze*. Wissenschaftliche Arbeiten der Fachrichtung Vermessungswesen der Universität Hannover, No. 88, 127 p.

———, 1981. Statistical Tests for Detecting Movements in Repeatedly Measured Geodetic Networks. *Tectonophysics*, Vol. 71, pp. 335-351.

Pelzer, H., 1971. Zur Analyse geodätischer Deformationsmessungen. *Deutsche Geodätische Kommission*, Series C, No. 164, Munich.

Strang van Hees, G. L., 1982. Variance-Covariance Transformations of Geodetic Networks. *Manuscripta Geodaetica*, Vol. 7, pp. 1-20.

(Received 5 December 1983; accepted 14 July 1984; revised 28 August 1984)

THE PHOTOGRAMMETRIC SOCIETY, LONDON

Membership of the Society entitles you to *The Photogrammetric Record* which is published twice yearly and is an internationally respected journal of great value to the practicing photogrammetrist. The Photogrammetric Society now offers a simplified form of membership to those who are already members of the American Society.

APPLICATION FORM

PLEASE USE BLOCK LETTERS

To: The Hon. Secretary,
The Photogrammetric Society,
Dept. of Photogrammetry & Surveying
University College London
Gower Street
London WC1E 6BT, England

I apply for membership of the Photogrammetric Society as,

☐ Member — Annual Subscription — $26.00
☐ Junior (under 25) Member — Annual Subscription — $13.00
☐ Corporate Member — Annual Subscription — $156.00

(Due on application and thereafter on July 1 of each year.)

(The first subscription of members elected after the 1st of January in any year is reduced by half.)
I confirm my wish to further the objects and interests of the Society and to abide by the Constitution and By-Laws. I enclose my subscription.

Surname, First Names ....
Age next birthday (if under 25) ....
Profession or Occupation ....
Educational Status ....
Present Employment ....
Address

....
ASP Membership ....
Card No. ....

Date .... Signature of Applicant ....

Applications for Corporate Membership, which is open to Universities, Manufacturers and Operating Companies, should be made by separate letter giving brief information of the Organisation's interest in photogrammetry.